Electronic Supplementary Material (ESI) for ChemComm.

Homolytic-cleavage of O-Cu(II) bond: XAFS and EPR spectroscopy evidence for one electron reduction of Cu(II) to Cu(I)

Hong Yi,[a] Guanghui Zhang,[a] Jie Xin,[a,] Yi Deng, Jeffrey T. Miller,[b,e] Arthur J. Kropf,[b]
Emilio E. Bunel,[b] Xiaotian Qi,[c] Yu Lan,[c] Jyh-Fu Lee,[d] Aiwen Lei* [a,b,f]

[a]College of Chemistry and Molecular Sciences, the Institute for Advanced Studies, Wuhan University, Wuhan, Hubei 430072, People's Republic of China.

[b]Chemical Sciences and Engineering Division, Argonne National Laboratory, 9700 South Cass Ave., Argonne, Illinois 60439, United States.

[c]School of Chemistry and Chemical Engineering, Chongqing University, Chongqing 400030, People's Republic of China.

[d]National Synchrotron Radiation Research Center, Hsinchu 30076, Taiwan

[e]School of Chemical Engineering, Purdue University, 480 Stadium Mall Dr., West Lafayette, Indiana 47907, United States.

[f]State Key Laboratory of Organometallic Chemistry, Shanghai Institute of Organic Chemistry, Chinese Academy of Sciences, 345 Lingling Road, Shanghai 200032, P. R. China

General Information

All reactions were run under an inert atmosphere on a Schlenk tube or in a glovebox, unless otherwise noted. All glassware was oven dried at 110 ^{o}C for more than 1 hour prior to use. N, N-dimethylformamide (DMF) was dried and distilled from calcium (II) hydride. Unless otherwise stated, commercially available reagents were used as received.

X-ray absorption measurements were acquired on the insertion device beam line of the Materials Research Collaborative Access Team (MRCAT) at the Advanced Photon Source, Argonne National Laboratory. The data were collected in transmission quick scan mode. Insertion device experiments utilized a cryogenically cooled double-crystal Si (111) monochromator in conjunction with an uncoated glass mirror to minimize the presence of harmonics. The monochromator was scanned continuously during the measurements with data points integrated over 0.5 eV for 0.03 s per data point. The ionization chambers were optimized for the maximum current with linear response (~10^{10} photons detected/sec) with 10% absorption (N_2) in the incident ion chamber and 70% absorption (60% N_2 and 40% Ar) in the transmission detector. A Cu foil spectrum (edge energy 8979 eV) was acquired simultaneously with each measurement for energy calibration and multiple scans were taken to ensure spectrum reproducibility (*1*).

Air sensitive samples were prepared in a glove box and placed in a sample holder made of PEEK (polyether ether ketone) equipped with a screw top and O-ring fitting prevent exposure to air and water (*2*). For solution samples, the Cu concentration was adjusted to be 0.05 - 0.1 M with a path length of 3.5 mm. Each solid sample was mixed with boron nitride to a weight ratio of 2% (Cu) in the glove box. The mixture was grinded well with pestle and then 25 mg of the mixture was packed into a solid sample tube with a radius of 2 mm. After sealed in a cell holder with Kapton windows, the cell holder was taken out of the glovebox and used for transmission mode measurement.

The edge energy of the X-Ray absorption near edge structure (XANES) spectrum was determined from the inflection point in the edge, i.e., the maximum in the first derivative of the XANES spectrum. The pre-edge energy was determined from the maximum of the pre-edge peak. Experimental phase shift, backscattering-amplitudes were used to fit the EXAFS data. Cu-O phase shift and back-scattering amplitude were obtained from reference compounds: Cu_2O (2 Cu-O at 1.85 Å) respectively (*3*). Background removal and normalization procedures were carried out using the Athena software package using standard methods (*4*). Standard procedures based on WinXAS 3.2 software were used to extract the extended X-ray absorption fine structure

(EXAFS) data (5). Fourier filtering technique was used to remove the features below 1 Å in the R-space spectra. The coordination parameters were obtained by a least square fit in R-space of the nearest neighbor, k^2-weighted Fourier transform data. The data fit equally well with both k^1 and k^3 weightings.

EPR spectra were recorded on a Bruker X-band A200 spectrometer. The samples were taken out into a small tube, and then recorded by EPR spectrometer at indicated temperature and parameter. The simulation software is Biomolecular EPR Spectroscopy Software.

For the React IR kinetic experiments, all spectra were recorded on a Mettler Toledo React IRTM 15 spectrometer using a diamond comb.

Experimental section

1. Reaction of $CuCl_2$ with ^{t}BuONa at room temperature

1.1 EPR experiment

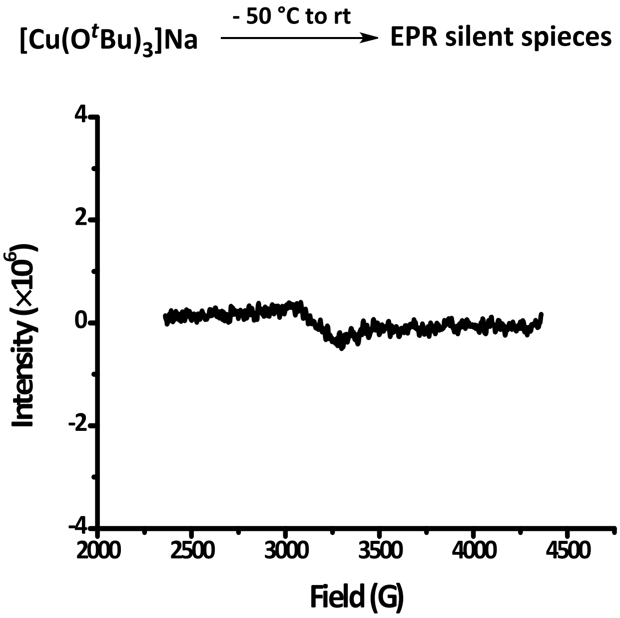

Fig. S1. EPR spectrum of the product of the reaction of $CuCl_2$ with excess ^{t}BuONa at room temperature

A three-neck reaction vessel was fitted with a magnetic stirring bar. The middle neck was used to take out the sample into a small tube for EPR analysis; the other two necks were capped by septa for injections and a nitrogen line. The reaction vessel was kept at room temperature. $CuCl_2$ (0.05 mmol) was added in the vessel. After evacuation under vacuum and flushing with nitrogen for three times, the three-neck vessel was charged with 4.0 mL dry DMF and excess ^{t}BuONa (0.5 mmol) was added. The reaction was stirred for 30 min and a solution sample was taken out into a small tube and then analyzed by EPR. EPR spectra were recorded at room temperature on EPR spectrometer operating at 9.419 GHz. Typical spectrometer parameters were: scan range, 2000 G; center field set, 3361 G; time constant, 40.96 ms; scan time, 20.48 s; modulation amplitude 1.0 G; modulation frequency 100 kHz; receiver gain $1.00*10^3$; microwave power, 19.68 mW.

1.2 XAS experiment

$CuCl_2$ + 10 ^{t}BuONa: In the glovebox, $CuCl_2$ (0.2 mmol) was added into a round bottom flask. ^{t}BuONa (2.0 mmol) was dissolved in 2.0 mL dry DMF and was then added to the flask at room temperature. After stirring for 30 mins, the solution was transferred to the solution cell and sealed, and then XAS spectra were taken.

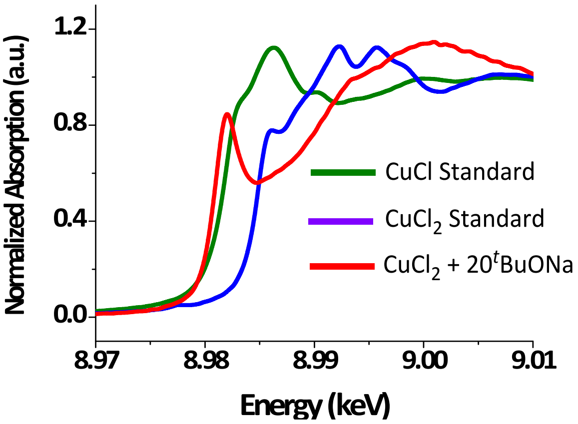

Fig. S2. XAFS spectra of ^{t}BuONa with $CuCl_2$ in DMF at room temperature

2. Reaction of $CuCl_2$ with ^{t}BuONa at -50 °C

2.1 IR experiment

$$CuCl_2 + {}^{t}BuONa \xrightarrow{-50\ ^{o}C} [Cu(O^{t}Bu)_3]Na$$

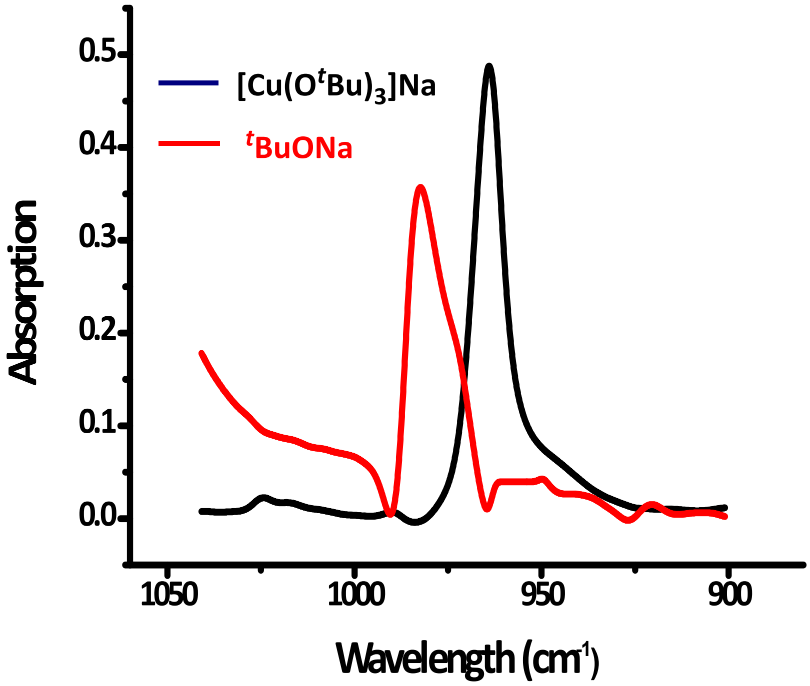

Fig. S3. IR spectra of ^{t}BuONa and [Cu(O^{t}Bu)$_3$]Na in DMF at -50 °C

In a dry three-neck reaction tube, 192 mg (2 mmol) NaO^{t}Bu was added. After evacuation under vacuum and flushing with nitrogen for three times, 4 mL DMF was injected into the tube. The absorption of NaO^{t}Bu at 985 cm^{-1} was observed. After the tube was cooled down to -50 ^{o}C, 67 mg (0.5 mmol) $CuCl_2$ was added. The absorption at 985 cm^{-1} decreased and a new peak at 962 cm^{-1} was formed.

2.2 XAS experiment

$$CuCl_2 + NaO^tBu \xrightarrow{-50\ °C} [Cu(O^tBu)_3]Na$$

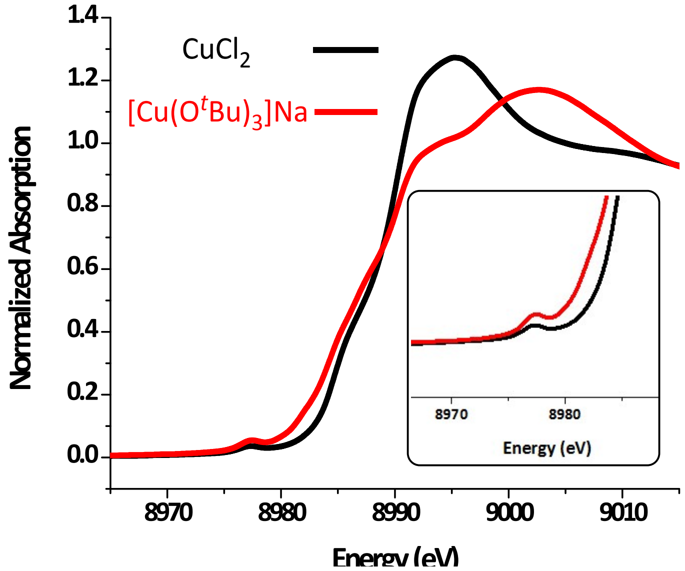

Fig. S4. XANES spectra of $CuCl_2$ and $[^tBuO)_3Cu]Na$ in DMF

$$CuCl_2 + NaO^tBu \xrightarrow{-50\ °C} [Cu(O^tBu)_3]Na$$

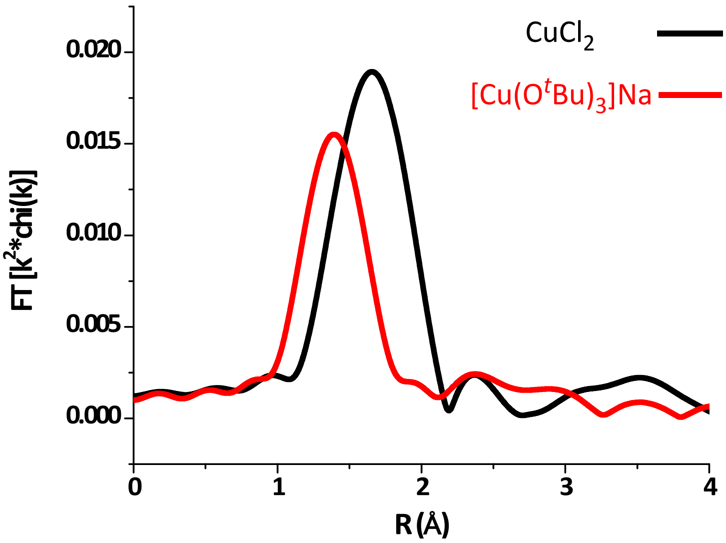

Fig. S5. k^2-weighted magnitude of the Fourier Transform ($CuCl_2$: FT: $2.73 < k < 11.03$ Å^{-1}; $[Cu(O^tBu)_3]Na$: FT: $2.51 < k < 11.57$ Å^{-1}).

In a glovebox, $CuCl_2$ (4 mmol) was dissolved in 20 mL dry DMF and then 1 mL of the solution was transferred into the XAS solution cell and sealed with the screw top. After it was taken out of the glovebox, the XAS spectrum of $CuCl_2$ DMF solution was taken at room temperature. ^{t}BuONa (20 mmol) was dissolved in 10 mL of dry DMF. After cooling down to -50 °C, 10 mL of $CuCl_2$ solution and 10 mL of ^{t}BuONa solution were combined and stirred at - 50 °C for 10 mins. After transferring the solution into a cold solution cell, XAS spectrum was taken at - 20 °C.

The pre-edge peak of the XANES spectra originates from the dipole-forbidden but quadrapole allowed 1s-3d transition (6). 3d electrons/orbitals are directly related to the oxidation state, so the pre-edge energy is usually used to determine the oxidation state of the 3d transition metals. The new Cu species has a pre-edge at 8977.5 eV which is in the typical range of Cu(II) species (Table S1). However, the shape of the XANES spectrum indicates that the new species has different coordination geometry. As is shown in the R-space spectra, the new species has a much shorter bond distance suggesting that no chloride was coordinated to Cu. It was determined to be 3-coordinate with an average bond distance of 1.86 Å by fitting of the R-space spectra. Similar Cu(II) ate complexes have been reported (*7, 8*). The bond distances that we obtained from XAS spectra are consistent with previously reported crystal structures.

2.3 EPR experiment

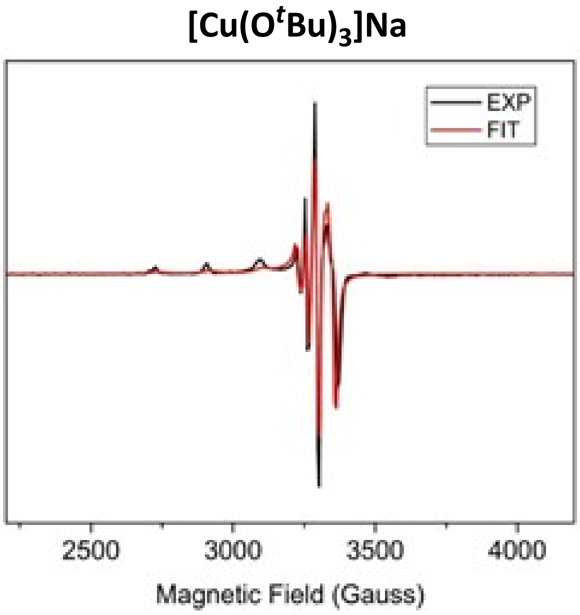

Fig. S6. Low tempersture spectrum (black) and fit of the EPR spectrum of [Cu(O^{t}Bu)$_3$]Na (red)

A three-neck reaction vessel was fitted with a magnetic stirring bar. The middle neck was used to take out the sample into a small tube for EPR analysis; the other two necks were capped by septa for injections and a nitrogen line. The reaction vessel was kept at -50 ^oC. $CuCl_2$ (0.05 mmol) was added in the vessel. After evacuation under vacuum and flushing with nitrogen for three times, the three-neck vessel was charged with 4.0 mL dry DMF. After the temperature was stable, excess ^{t}BuONa (0.5 mmol) was added. The solution sample was taken out into a small tube, frozen by liquid nitrogen and then analyzed by EPR. EPR spectra was recorded at 160K on EPR spectrometer operating at 9.419 GHz. Typical spectrometer parameters were: scan range, 2000 G; center field set, 3361 G; time constant, 40.96 ms; scan time, 20.48 s; modulation amplitude 1.0 G; modulation frequency 100 kHz; receiver gain $1.00*10^3$; microwave power, 19.68 mW.

The assignment as a mononuclear species was confirmed by simulation of the spectrum which resulted in spin Hamiltonian parameters: $g_x = 2.001$, $g_y = 2.001$, $g_z = 2.242$ and $A_x = 37$ G, $A_y = 25$ G, $A_z = 197$ G.

3. *In-situ* XAFS experiment and *in-situ I*R experiment

3.1 XAS experiment

In a glovebox, $CuCl_2$ (4 mmol) was dissolved in 20 mL dry DMF and then the solution was transferred into the XAS solution cell and sealed with the screw top. After taken out of the glovebox, the XAS spectrum of $CuCl_2$ DMF solution was taken at room temperature. ^{t}BuONa (20 mmol) was dissolved in 10 mL of dry DMF. After cooling down to -50 °C, 10 mL of $CuCl_2$ solution and 10 mL of ^{t}BuONa solution were combined and stirred at - 50 °C for 10 mins. After transferring the solution into a cold solution cell, the solution was warmed up to room temperature and XAS spectra were taken simultaneously to track the reduction process.

3.2 IR experiment

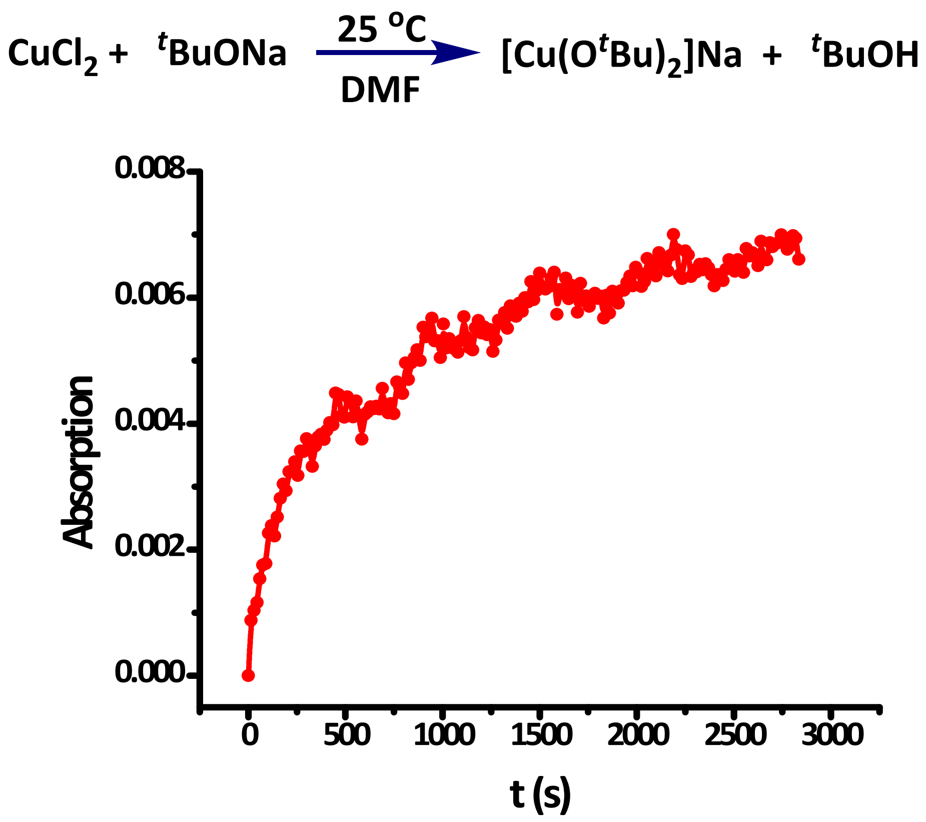

Fig. S7. Kinetic profile of the reaction of $CuCl_2$ with excess ${}^tBuONa$ at room temperature

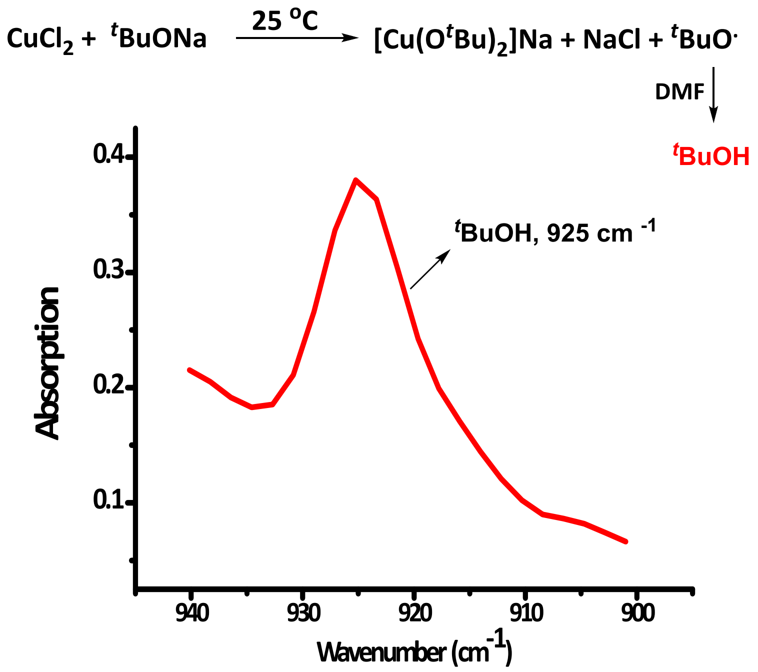

Fig. S8. IR spectrum of ${}^tBuOH$ observed in the reaction $CuCl_2$ with excess ${}^tBuONa$ at room temperature

In a dry three-neck reaction tube, 192 mg (5.0 mmol) NaO^{t}Bu was added. After evacuation under vacuum and flushing with nitrogen for three times, 4 mL DMF was injected into the tube. Then reaction was monitored by IR at room temperature. When 67 mg (0.5 mmol) $CuCl_2$ was added into the solution, the absorption of ^{t}BuOH at 925 cm^{-1} was increased, and the kinetic profile is shown above.

Table S1 Edge Energy and Oxidation States

Sample	**Edge Energy (eV)**	**Oxidation State**	**Comment**
Cu foil	8979.0	0	Reference
Cu_2O (solid)	8980.2	+1	Reference
CuCl (Solid)	8981.9	+1	Reference
CuI (solid)	8981.7	+1	Reference
$CuCl_2$ (solid)	8978.0 (pre-edge)	+2	Reference
$CuCl_2$ (DMF solution)	8977.2 (pre-edge)	+2	Reference
[Cu(O^{t}Bu)$_2$]Na (DMF solution)	8980.9	+1	
[Cu(O^{t}Bu)$_3$]Na (	8977.2 (pre-edge)	+2	

Table S2 EXAFS First Shell Fitting Results

Sample	**Scatterer**	**Coordination number**	**Bond distance (Å)**	**σ^2**	**ΔE_0 (eV)**
[Cu(O^{t}Bu)$_3$]Na (DMF solution)	**Cu-O**	**3.0**	**1.86**	**0.003**	**-7.52**
[Cu(O^{t}Bu)$_2$]Na (DMF solution)	**Cu-O**	**2.2**	**1.82**	**0.001**	**2.91**

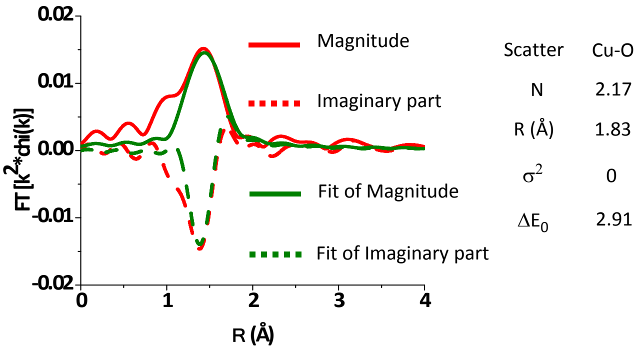

Fig. S9. R-space spectra and fitting results (3.08 < k < 11.80 Å-1 and 1.08 < R < 1.83 Å), EXAFS spectra of reactions between 20 eq of ^{t}BuONa with CuCl$_2$ in DMF. N = coordination number, E$_0$ = threshold energy, and σ^2 is Debye-Waller factor. Estimated uncertainties are ± 0.02 Å for R and ± 0.25 for N.

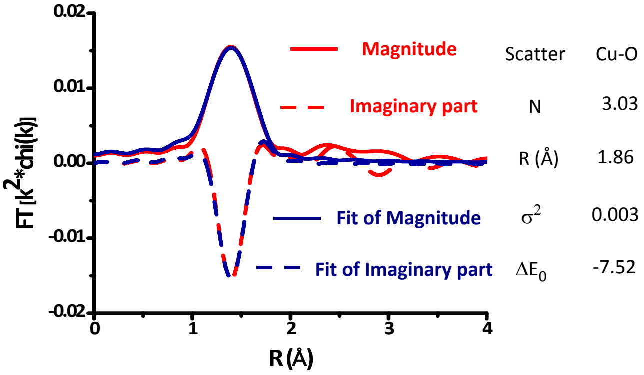

Fig. S10. Fitting results of the R-Space EXAFS spectrum of [Cu^{II}(O^{t}Bu)$_3$]Na (FT: 2.51 - 11.55 Å-1, fitting range: 1.00 - 1.79 Å; CN: coordination number, R: bond distance, E$_0$ = threshold energy, and σ^2 is Debye-Waller factor).

4. DFT calculation

4.1. Complete Reference for Gaussian 09

Gaussian 09, Revision D.01, Frisch, M. J.; Trucks, G. W.; Schlegel, H. B.; Scuseria, G. E.; Robb, M. A.; Cheeseman, J. R.; Scalmani, G.; Barone, V.; Mennucci, B.; Petersson, G. A.; Nakatsuji, H.; Caricato, M.; Li, X.; Hratchian, H. P.; Izmaylov, A. F.; Bloino, J.; Zheng, G.; Sonnenberg, J. L.; Hada, M.; Ehara, M.; Toyota, K.; Fukuda, R.; Hasegawa, J.; Ishida, M.; Nakajima, T.; Honda, Y.; Kitao, O.; Nakai, H.; Vreven, T.;

Montgomery, Jr., J. A.; Peralta, J. E.; Ogliaro, F.; Bearpark, M.; Heyd, J. J.; Brothers, E.; Kudin, K. N.; Staroverov, V. N.; Kobayashi, R.; Normand, J.; Raghavachari, K.; Rendell, A.; Burant, J. C.; Iyengar, S. S.; Tomasi, J.; Cossi, M.; Rega, N.; Millam, N. J.; Klene, M.; Knox, J. E.; Cross, J. B.; Bakken, V.; Adamo, C.; Jaramillo, J.; Gomperts, R.; Stratmann, R. E.; Yazyev, O.; Austin, A. J.; Cammi, R.; Pomelli, C.; Ochterski, J. W.; Martin, R. L.; Morokuma, K.; Zakrzewski, V. G.; Voth, G. A.; Salvador, P.; Dannenberg, J. J.; Dapprich, S.; Daniels, A. D.; Farkas, Ö.; Foresman, J. B.; Ortiz, J. V.; Cioslowski, J.; Fox, D. J. Gaussian, Inc., Wallingford CT, **2013**.

4.2. Calculated free energy for the reduction of $[Cu^{II}(O^tBu)_3]^-$ to $[Cu^{I}(O^tBu)_2]^-$

$$[\mathbf{Cu^{II}(O^{\mathit{t}}Bu)_3}]^- \xrightarrow{\Delta G = 9.6\ \text{kcal/mol}} [\mathbf{Cu^{I}(O^{\mathit{t}}Bu)_2}]^- + {}^\bullet\mathbf{O^{\mathit{t}}Bu}$$

Density functional theory (DFT) calculation was employed to study the reduction of $[Cu^{II}(O^tBu)_3]^-$ to provide further support for the experiment. As shown above, the reaction free energy is calculated to be 9.6 kcal/mol endothermic, which indicates the reduction is a feasible process.

4.3. Absolute Calculation Energies, Enthalpies, and Free Energies

All the DFT calculations were carried out with the GAUSSIAN 09 series of programs. DFT method B3-LYP (9) with a standard 6-31G(d) basis set (lanl2dz basis set for Cu) was used for geometry optimizations. Harmonic frequency calculations were performed for all stationary points to confirm them as a local minima or transition structures and to derive the thermochemical corrections for the enthalpies and free energies. The SCS-MP2 (10) method is used to calculate single point energies to give more accurate energy information. The larger basis set aug-cc-pvtz is employed in the single point calculations for all the atoms.

Geometry	$E_{(\text{elec-B3LYP})}{}^{a}$	$E_{(\text{elec-SCS-MP2})}{}^{b}$	$G_{(\text{corr-B3LYP})}{}^{c}$	$H_{(\text{corr-B3LYP})}{}^{d}$	IF^{e}
$[\mathrm{Cu^{II}(O}^t\mathrm{Bu)_3}]^-$	-895.437878	-2338.103544	0.321580	0.399925	-
$[\mathrm{Cu^{I}(O}^t\mathrm{Bu)_3}]^-$	-662.382807	-2105.440648	0.205177	0.266119	-
^{t}BuO’	-233.001933	-232.624611	0.093477	0.130528	-

[a]The electronic energy calculated by B3LYP in gas phase. [b]The electronic energy calculated by SCS-MP2 in gas phase. [c]The thermal correction to Gibbs free energy calculated by B3LYP in gas phase. [d]The thermal correction to enthalpy calculated by B3LYP in gas phase. [e]The B3LYP calculated imaginary frequencies for the transition states.

4.4. Optimized Geometries for All the Compounds and Transition States

$[\mathrm{Cu^{II}(O}^t\mathrm{Bu)_3}]^-$

Cu	-0.02599200	-0.32106300	-0.30565200
O	1.81318800	-0.49339200	-0.66838100
O	-1.53587100	-1.40745500	-0.38440700
O	-0.70513800	1.41325300	0.14753400
C	-2.83022000	-1.14357400	0.06407500
C	0.07590800	2.56700700	0.03924900
C	2.74752700	-1.23645500	0.05108700
C	2.94873100	-2.59864700	-0.65595100
H	1.99963900	-3.14739900	-0.67355500
H	3.25931700	-2.43160800	-1.69411500
H	3.70643900	-3.22360100	-0.16044400
C	4.09000100	-0.46708600	0.06060100
H	3.96389600	0.49976300	0.56165500
H	4.88995400	-1.02152400	0.57251300
H	4.40726800	-0.27079400	-0.97034800
C	2.29654900	-1.49005100	1.50893700
H	2.13883300	-0.53673700	2.02683300
H	1.34642600	-2.03964200	1.51879400
H	3.03453700	-2.07386200	2.07811100
C	1.16491700	2.60200400	1.13634800
H	0.69801000	2.50159200	2.12407100
H	1.84828200	1.75938500	0.98950600
H	1.75023500	3.53347800	1.11975300
C	-0.88367900	3.76442500	0.23355900

H	-0.35791600	4.72869700	0.18232300
H	-1.65927600	3.74698700	-0.54098400
H	-1.37952200	3.68761900	1.20849100
C	0.74919700	2.66637100	-1.34943700
H	1.42977500	1.81837100	-1.48603000
H	-0.01745300	2.62829400	-2.13364200
H	1.31996100	3.59964600	-1.46795400
C	-3.48630200	-0.05939100	-0.82211100
H	-2.87673000	0.84754400	-0.76669700
H	-3.51435500	-0.40215100	-1.86461100
H	-4.51449800	0.17220000	-0.50535500
C	-2.81655800	-0.66413500	1.53425300
H	-3.82885600	-0.46744600	1.91813900
H	-2.35219900	-1.43090000	2.16859400
H	-2.22385000	0.25384800	1.60090000
C	-3.62855400	-2.46217700	-0.04554600
H	-3.15704100	-3.23672000	0.57177800
H	-4.67096000	-2.34064300	0.28264800
H	-3.62869600	-2.81258400	-1.08481200

[Cu^{I}(O^{t}Bu)$_2$]$^-$

O	-1.78368900	-0.68909700	0.46509100
C	-2.78184200	0.15350100	0.01061200
C	-2.90956000	0.10904700	-1.53390600
H	-1.96867300	0.44298200	-1.98842300
H	-3.08663100	-0.92438700	-1.85684900
H	-3.72754200	0.73972100	-1.91595300
C	-2.52438600	1.61902600	0.44755900
H	-3.32797500	2.30771700	0.14321000
H	-2.42313400	1.66152100	1.53902200
H	-1.58051300	1.96800200	0.01133300
C	-4.11794800	-0.32376900	0.63440700
H	-4.03733800	-0.30482200	1.72795600
H	-4.97593400	0.29650800	0.33485000
H	-4.31347600	-1.35978200	0.33202800
Cu	0.00003300	-0.59736900	0.00002200
O	1.78385600	-0.68956700	-0.46464600
C	2.78182300	0.15349400	-0.01060200
C	2.52455400	1.61857500	-0.44914000
H	1.58058400	1.96805600	-0.01353100
H	3.32810000	2.30753500	-0.14528500
H	2.42359800	1.65994600	-1.54067300
C	2.90893100	0.11059900	1.53401000
H	3.08588500	-0.92250600	1.85806900

H	3.72675800	0.74166500	1.91574400
H	1.96786500	0.44497900	1.98782500
C	4.11817900	-0.32440800	-0.63337100
H	4.97605000	0.29615100	-0.33407100
H	4.31355900	-1.36012500	-0.32988700
H	4.03801800	-0.30653300	-1.72697100

^{t}BuO’

O	0.70223405	-1.58482649	0.00000000
C	2.05932842	-1.35249684	0.38628721
C	2.71747346	-0.38026921	-0.61031629
H	2.61783573	0.62208852	-0.24941285
H	3.75501786	-0.62142695	-0.71153175
H	2.23684918	-0.46596070	-1.56244930
C	2.09333170	-0.74046189	1.79903523
H	1.23980570	-1.07261626	2.35226831
H	2.98620455	-1.05043731	2.30062600
H	2.07761049	0.32691284	1.72579562
C	2.82866574	-2.68655834	0.38614406
H	3.84420385	-2.51266541	0.67483695
H	2.37159832	-3.36194276	1.07885269
H	2.80473437	-3.11197932	-0.59535698

References

1. J. A. Bearden, A. F. Burr, Reevaluation of X-Ray Atomic Energy Levels. *Rev. Mod. Phys.* **39**, 125 (1967).
2. R. C. Nelson, J. T. Miller, An introduction to X-ray absorption spectroscopy and its in situ application to organometallic compounds and homogeneous catalysts. *Catal. Sci. Technol.* **2**, 461 (2012).
3. R. Restori, D. Schwarzenbach, Charge density in cuprite, Cu2O. *Acta Crystallogr., Sect. B: Struct. Sci.* **42**, 201 (1986).
4. B. Ravel, M. Newville, ATHENA, ARTEMIS, HEPHAESTUS: data analysis for X-ray absorption spectroscopy using IFEFFIT. *J. Synchrotron Rad.* **12**, 537 (2005).
5. T. Ressler, WinXAS: a Program for X-ray Absorption Spectroscopy Data Analysis under MS-Windows. *J. Synchrotron Rad.* **5**, 118 (1998).
6. T. Yamamoto, Assignment of pre-edge peaks in K-edge x-ray absorption spectra of 3d transition metal compounds: electric dipole or quadrupole? *X-Ray Spectrom.* **37**, 572 (2008).
7. R. Becker, J. Weiß, M. Winter, K. Merz, R. A. Fischer, New heterometallic copper zinc alkoxides: synthesis, structure properties and pyrolysis to Cu/ZnO composites. *J. Organomet. Chem.* **630**, 253 (2001).
8. A. P. Purdy, C. F. George, J. H. Callahan, New alkoxides of copper and the alkaline and alkaline-earth metals. Crystal structure of Na2Cu[OCH(CF3)2]4. *Inorg. Chem.* **30**, 2812 (1991).

9 (a) Lee, C.; Yang, W.; Parr, R. G. *Phys. Rev. B* **1988**, *37*, 785; (b) Becke, A. D. *J. Chem. Phys.* **1993**, *98*, 5648-5652.

10 (a) Grimme, S. *J. Chem. Phys.* **2003**, *118*, 9095-9102; (b)Neese, F.; Hansen, A.; Wennmohs, F. and Grimme, S. *Acc. Chem. Res.* **2009**, *42*, 641-648.